The Mechanics of Large Bubbles Rising through Extended Liquids and through Liquids in Tubes

Part I and Part II

Sir Geoffrey Ingram Taylor (* 7 March 1886, †27 June 1975)
Rhisiart Morgan Davies (* 4 Februar 1903, †18 Februar 1958)

Proceedings of the Royal Society A
1950

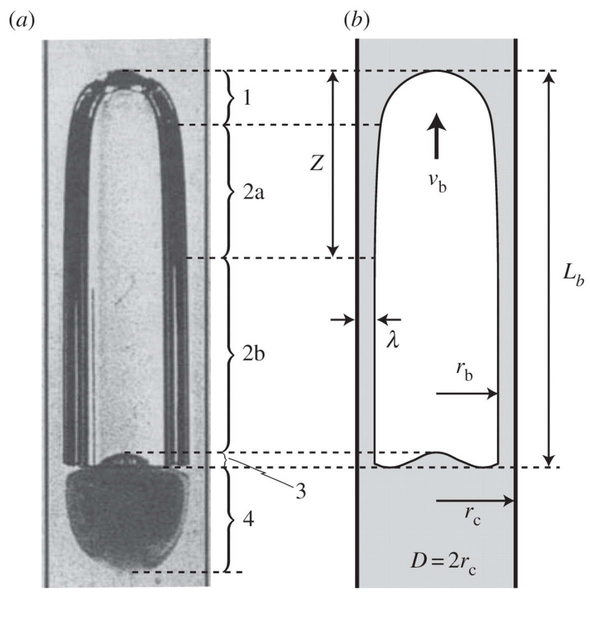

THE ROYAL SOCIETY
6-9 Carlton House Terrace, London SW1Y 5AG

Part I describes measurements of the shape and rate of rise of air bubbles varying in volume from 15 to 200 cm.[3] when they rise through nitrobenzene or water.

Measurements of photographs of bubbles formed in nitrobenzene show that the greater part of the upper surface is always spherical. A theoretical discussion, based on the assumption that the pressure over the front of the bubble is the same as that in ideal hydrodynamic flow round a sphere, shows that the velocity of rise, U, should be related to the radius of curvature, R, in the region of the vertex, by the equation $U = \frac{2}{3} \cdot \sqrt{g \cdot R}$; the agreement between this relationship and the experimental results is excellent.

For geometrically similar bubbles of such large diameter that the drag coefficient would be independent of Reynolds's number, it would be expected that U would be proportional to the sixth root of the volume, V; measurements of eighty-eight bubbles show considerable scatter in the values of $U/V^{\frac{1}{6}}$, although there is no systematic variation in the value of this ratio with the volume.

Part II. Though the characteristics of a large bubble are, associated with the observed fact that the hydrodynamic pressure on the front of a spherical cap moving through a fluid is nearly the same as that on a complete sphere, the mechanics of a rising bubble cannot be completely understood till the observed pressure distribution on a spherical cap is understood. Failing this, the case of a large bubble running up a circular tube filled with water and emptying at the bottom is capable of being analyzed completely because the bubble is not then followed by a wake. An approximate calculation shows that the velocity U of rise is $U = 0.46 \cdot \sqrt{g \cdot a}$, where a is the radius of the tube. Experiments with a tube 7.9 cm. diameter gave values of U from 29.1 to 30.6 cm./sec., corresponding with values of $U/\sqrt{g \cdot a}$ from 0.466 to 0.490.

Contents

1 PART I. DEDUCING THE RISE OF GAS BUBBLES

1.1 INTRODUCTION AND EXPERIMENTAL METHOD

The rise of gas bubbles in liquids has been studied by several workers (Allen 1900; Hoefer 1913; Miyagi 1925, 1929), but in all the work so far published the bubbles have been so small that the results are not applicable to the study of the rise of large volumes of gas, such as those produced in submarine explosions. In the experiments here described, bubbles ranging in volume from 1.5 to 34 cm.^{3} were formed in nitrobenzene contained in a tank, 2 ft. $\times$ 2 ft. $\times$ 2 ft. 6 in., filled to a depth of about 2 ft. with the liquid. The bubbles were photographed by spark photography at intervals of about 10 msec. (1 msec. = 10^{-3} sec.), using a revolving drum camera, and appropriate spark timing. In some further experiments, bubbles covering a range of volume from 4.5 to 200 cm.^{3} were formed in a cylindrical tank, 2 ft. 6 in. diameter, filled with water to a depth of 3ft. 6 in., and their mean velocity of rise over a measured distance was determined. In both sets of experiments, the air volume was determined by collecting the bubble in a graduated glass cylinder.

Considerable difficulty was found in producing single, large bubbles of gas, and the method finally adopted was to pivot an inverted beaker containing air, which was then tilted so that the air was released. In general, the air is released from the beaker in a stream of bubbles of varying sizes, but by adjusting the rate of tilting, it was found possible to arrange that the air was spilled into a single bubble.

Two successive photographs of a typical bubble formed in this way in nitrobenzene are shown in figure 1.1, the time interval between the two photographs being 10.3 msec. In addition to the bubble, the photographs show a steel ball, $\frac{1}{4}$ in. diameter, soldered at the lower end of a vertical rod immersed in the liquid; this arrangement was used to find the scale of the photographs and to give a reference mark from which the vertical displacement of the bubble could be measured.

The uniformity of the velocity of rise of the bubbles may be judged by figure 1.2, in which time, t, and the vertical displacement, X,of two bubbles are plotted as abscissae and ordinates, respectively. The actual measured values of X and t for the bubble of figure 1.1 are indicated by the circular dots in figure 1.2, and those for a second, larger bubble by crosses; the straight lines

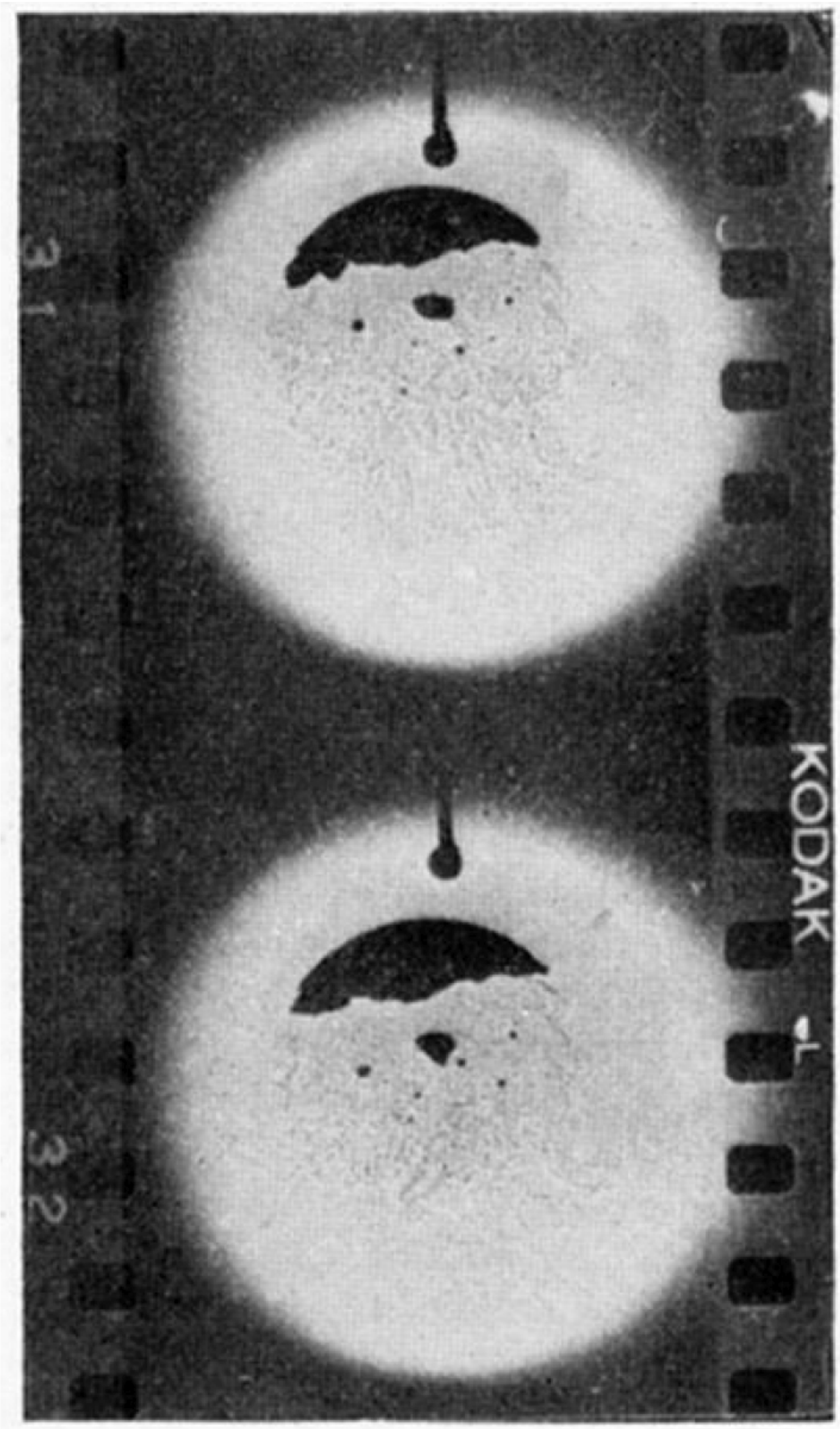

Figure 1.1
Successive spark photographs of an air-filled bubble rising in nitrobenzene. Time interval between photographs = 10.3 msec. Velocity of rise of bubble = 36.7 cm./sec. Diameter of steel ball in the upper part of the photographs $= \frac{1}{4}$ *in.*

of closest fit drawn through the observed points are denoted by A and B respectively. It will be seen that the scatter of the experimental points is not excessive, and that the velocity of rise, U, of the two bubbles is reasonably constant over the interval measured.

The shape of the profile of the bubbles was found by measuring the films on a travelling microscope fitted with two independent motions at right angles to one another. The results for the lower photograph of figure 1.1 are shown graphically in figure 1.3, where the circular dots represent points on the central, regular portion of the profile of the bubble, deduced from the microscope readings. In figure 1.3, the vertical and horizontal axes are parallel to the corresponding axes in the tank, and the origin is taken at the uppermost point on the bubble; the dimensions given refer to the actual size of the bubble. The crosses with vertical axes and with axes at 45° to the vertical in figure 1.3 represent points on the profile of the same bubble, obtained from measurements of photographs taken 105.7 and 132.5 msec. earlier than the lower photograph of figure 1.1. The agreement between the three sets of points shows that the shape of the cap of the bubble undergoes very little variation over the range of time covered by the three photographs.

The curve in figure 1.3 is an arc of circle of radius 3.01 cm., drawn to pass through the origin, and since the scatter of the observed points around this curve is within the limits of the errors made in measuring the film, the upper part of the bubble is a portion of a sphere within the experimental error. It is worth noticing that the angle subtended at the centre of the circle by the arc in figure 1.3 is about 75°, whilst the angular width of the whole bubble in figure 1.1 (referred to the centre) is about 90°.

1.2 EXPLANATION OF WHY THE TOP OF LARGE BUBBLES IS SPHERICAL

The perfection of the spherical shape of the top of the bubble led us to consider the condition which must be satisfied at its surface. The pressure there may be taken as constant, for the variations in pressure through the interior air must be so small as to be negligible. The pressure in the fluid outside the bubble is due to the dynamics of the flow round it, and to gravity. The condition that the pressure at the surface of the bubble is constant requires that these two causes shall neutralize one another. Applying Bernoulli's equation to steady flow relative to the bubble, which is assumed to be symmetrical so that the relative velocity at its highest point is zero, the surface condition is

$$q^2 = 2 \cdot g \cdot x \,, \tag{1.1}$$

where x is the depth below the highest point, q the fluid velocity relative to the bubble and g is the acceleration of gravity.

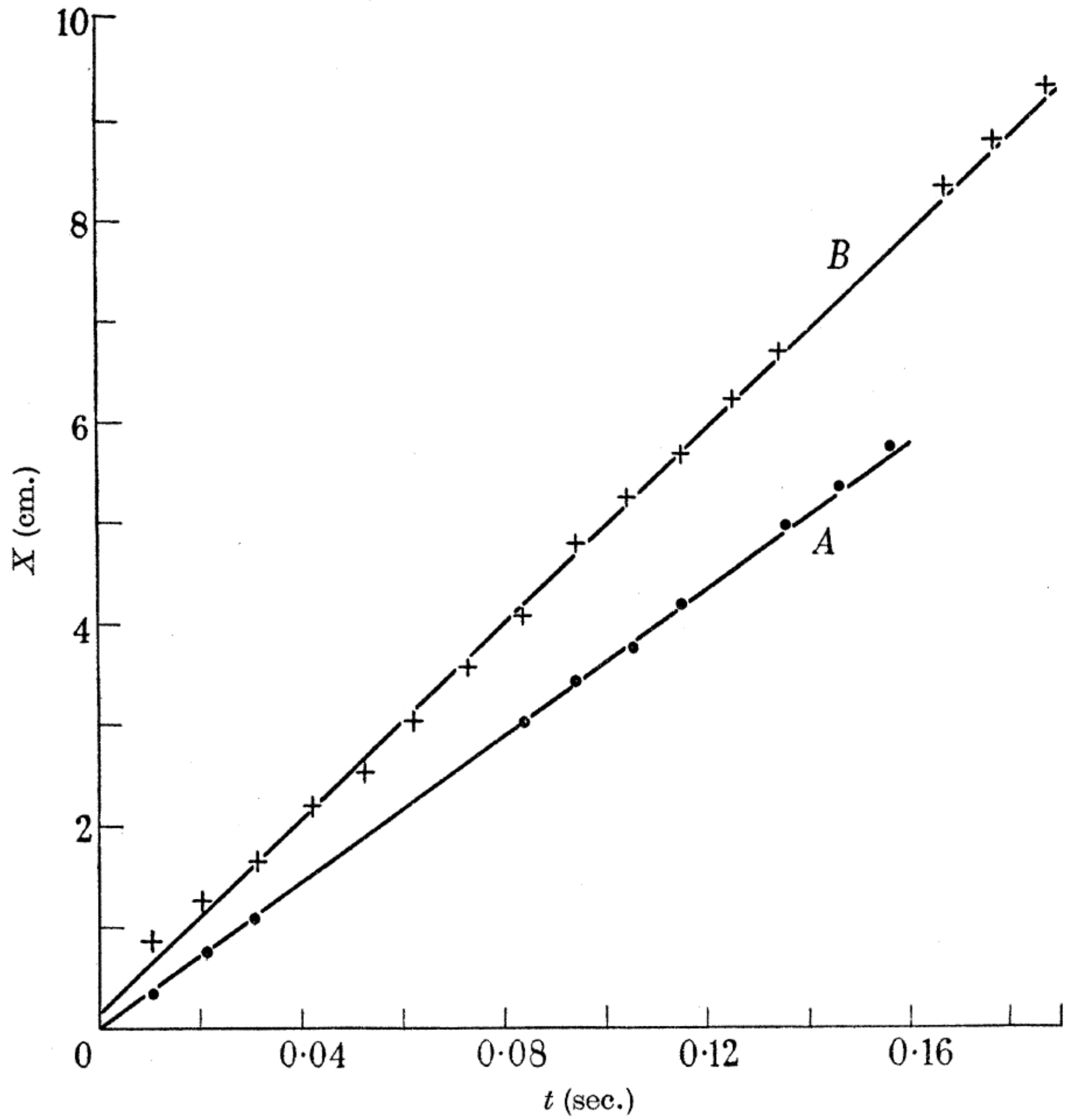

Figure 1.2
(Displacement, time) curves deduced from photographs of rising bubbles. • and + Experimental values; curve A, U = 36.7 cm./sec.; curve B, U = 48.2 cm./sec.

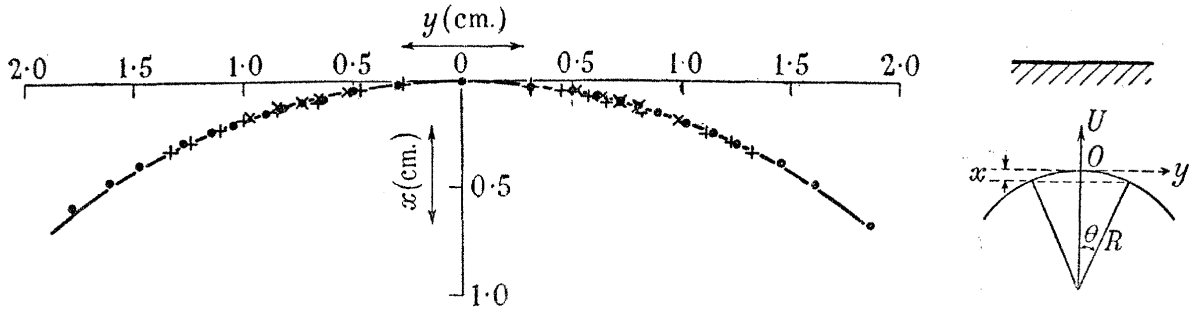

Figure 1.3
Shape of the profile of a bubble. • Bubble shown in the lower photograph of figure 1.1; + the same bubble 0.106 sec. earlier; × the same bubble 0.133 sec. earlier; — an arc of circle of radius 3.01 cm.

The bubbles were observed to be spherical above and more or less flat beneath. It is not possible to calculate the flow round such a shape. Recourse was therefore had to experiment. Three models were made in brass, each had a spherical surface 1 in. radius and a flat under-surface. Small pressure holes were bored in both surfaces of each model. They were set up in a wind tunnel and the pressure distribution determined at a wind speed of 15 m./sec. The angles, θ_m, between the polar axes of the models and the radii to their rims were 75°, 55° and 30°, a range which more than covered the values observed in bubbles. The results are given in non-dimensional form in figure 1.4, when $(p_\theta - p_0)/\frac{1}{2}\rho U^2$ is plotted against θ, the angle which the radius from the centre of the sphere makes with the polar axis. Here p_θ is the pressure at angle θ, p_0 that at the vertex and $\frac{1}{2}\rho U^2$ the pitot pressure in the tunnel. It has long been known that when a sphere is set up in a wind tunnel, the pressure distribution over a large part of the windward side is rather nearly the same as the theoretical distribution of pressure over a sphere obtained by classical methods using velocity potential.
This is true even though the flow behind the sphere bears no relationship to the theoretical flow. For this reason the theoretical pressure distribution round a complete sphere was calculated from the well-known expression

$$\frac{q^2}{U^2} = \frac{p_0 - p_\theta}{\frac{1}{2}\rho U^2} = \frac{9}{4}\sin^2\theta\,, \tag{1.2}$$

and shown in figure 1.4. It will be seen that the measured distributions over all the lenticular bodies are rather close to the theoretical distribution for a sphere in the range $0 < \theta < 20°$. The 55° and 75° bodies retain this property nearly out to their edges, but the drop in pressure below that at the vertex at any point is rather less than the theoretical value.

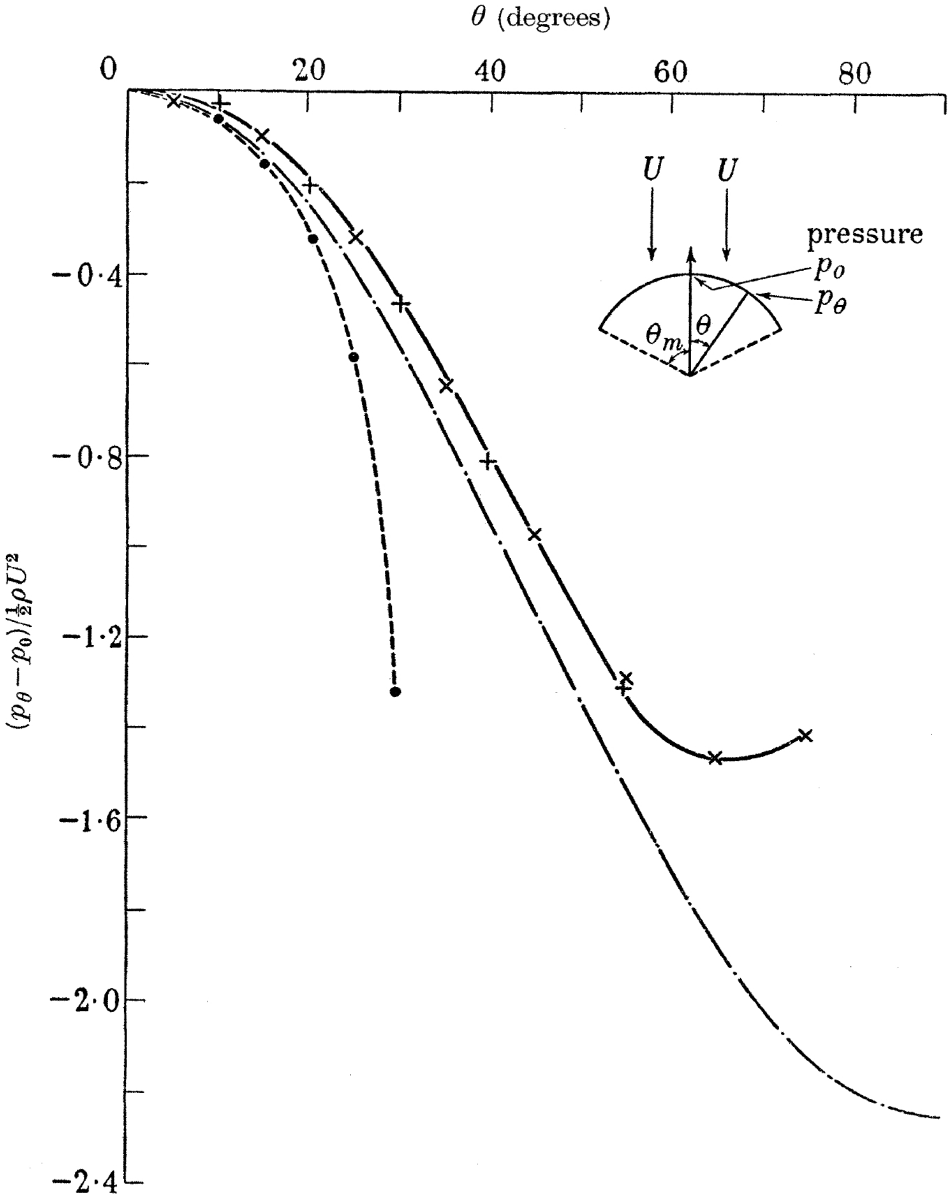

Figure 1.4
The variation of pressure over the surfaces of lenticular bodies in a wind tunnel. Experimental values: • $\theta_m = 30°$; + $\theta_m = 55°$; × $\theta_m = 75°$; · — · — · theoretical curve for a sphere, assuming ideal fluid flow.
Mean pressures p_b on the backs of the bodies:

θ_m	30°	55°	75°
$(p_b - p_0)/\frac{1}{2}\rho U^2$	-1.32	-1.39	-1.41

The observed values of $(p_0 - p_\theta)/\frac{1}{2}\rho U^2$, which may be equated to q^2/U^2, have been taken from the faired curve for $\theta_m = 55°$ and $75°$ in figure 1.4, and their values are given in the first row of table 1.1. In the next row are tabulated the values of $x/R = 1 - \cos\theta$, where R is the radius of the spherical surface of the lenticular body. Below these are given the values of $q^2/U^2 \cdot (1 - \cos\theta) = q^2 R/U^2 x$. It will be seen that this ratio is nearly constant, its mean value being 3.28.

The condition (1.1) that bubbles of lenticular shape may have constant pressure over their spherical surfaces is satisfied if $q^2 R/U^2 x = 3.28$ is identical with $q^2 = 2gx$. Eliminating x/q^2

$$U^2 = 2 \cdot g \cdot R/3.28 = 0.61 \cdot g \cdot R \quad \text{or} \quad U = 0.78 \cdot \sqrt{g \cdot R} \tag{1.3}$$

If the pressure had been exactly the same as the calculated pressure over a complete sphere, the condition (1.1) could be satisfied over the portion near the stagnation point only, for in that case $q^2 = \frac{9}{4}U^2 \sin^2\theta$ and $x = R \cdot (1 - \cos\theta)$, so that $q^2/x = 2g$ if

$$\frac{U^2}{g \cdot R} = \frac{8}{9} \cdot \left(\frac{1 - \cos\theta}{\sin^2\theta}\right) .$$

When θ is small, $(1 - \cos\theta)/\sin^2\theta \to \frac{1}{2}$, so that the pressure condition would be satisfied near the stagnation point, i.e.

$$U^2 = \frac{4}{9} \cdot g \cdot R \quad \text{or} \quad U = \frac{2}{3} \cdot \sqrt{g \cdot R}\,. \tag{1.4}$$

1.3 COMPARISON WITH OBSERVATION

Fourteen bubbles, rising in nitrobenzene, were photographed. The results of the measurement of the films are summarized in table 1.2, where the first three columns give the volume V of the bubbles, the radius of curvature R and the velocity of rise U. The fourth column gives the maximum transverse dimension $2A$, and the fifth column $\theta_m = \sin^{-1} A/R$. The sixth column gives the drag coefficient, C_D, of the bubble calculated from the equation

θ	15°	20°	25°	30°	35°	40°	45°
$\frac{q^2}{U^2} = \frac{p_0 - p_\theta}{\frac{1}{2}\rho U^2}$	0.10	0.192	0.315	0.465	0.628	0.805	0.975
$1 - \cos\theta$	0.0341	0.0603	0.0937	0.1340	0.1808	0.2340	0.2929
$\frac{q^2}{U^2 \cdot (1-\cos\theta)}$	2.94	3.18	3.25	3.44	3.47	3.44	3.33

Mean value of $\frac{q^2}{U^2 \cdot (1-\cos\theta)}$ = 3.28

Table 1.1
Observed values of $(p_0 - p_\theta)/\frac{1}{2}\rho U^2$ *and values of* $x/R = 1 - \cos\theta$

volume V (cm.^{3})	radius of curvature R (cm.)	velocity U (cm./sec.)	maximum transverse dimension, $2A$ (cm.)	$\theta_m = \sin^{-1} A/R$	drag coef- ficient C_D	Reynolds number Re
1.48	2.41	29.2	2.86	36.4	0.53	2780
3.50	2.09	29.6	3.14	48.6	1.02	3090
4.06	2.04	28.9	3.48	58.3	1.00	3360
4.31	2.17	28.0	3.16	46.8	1.37	2950
6.40	2.78	35.5	4.98	63.6	0.52	5900
7.30	2.65	34.2	4.40	56.1	0.80	5010
8.02	2.67	34.0	4.23	52.5	0.97	4790
–	3.01	36.7	–	–	–	–
8.80	3.17	37.2	5.26	56.1	0.58	6520
9.18	2.77	33.0	4.53	55.8	1.00	5020
18.40	3.30	37.3	5.10	50.7	1.27	6340
21.25	3.51	38.1	5.85	56.5	1.07	7440
28.1	4.16	43.0	–	–	–	–
33.8	4.27	42.1	6.19	46.5	1.25	8700
–	4.84	48.2	–	–	–	–

Table 1.2
Bubbles in Nitrobenzene

$$C_D \cdot \pi A^2 \cdot \frac{1}{2}\rho U^2 \,. \tag{1.5}$$

The last column gives the Reynolds number Re

$$Re = \frac{U \cdot A}{\nu} \tag{1.6}$$

The viscosity of nitrobenzene is 0.018 poise at 14 °C and the density is 1.2 g./cm.^{3}, so that $\nu =$ 0.015 cm.^{2}/sec.
The experimental values of U are plotted against $\sqrt{R}$ in figure 1.5. It will be seen that they lie closely scattered round the line $U = \frac{2}{3} \cdot \sqrt{g \cdot R}$ and well below the line $U = 0.78 \cdot \sqrt{g \cdot R}$.
It is curious that the experiments agree better with the arbitrary assumption that flow over the forward part of the bubble is the same as that calculated for a sphere moving in a frictionless liquid than with calculations based on

the pressure distribution measured over the surface of a solid of nearly the same shape as the bubble.
It will be noted, however, that the flow of the liquid near the front of a bubble would be expected to be more nearly a truly irrotational one than that near a solid body, because in the latter case a boundary layer would necessarily be present, whereas in the former the air in the bubble would cause no appreciable drag so that no boundary layer would be formed. The closeness with which the observed points fit the line $U = \frac{2}{3} \cdot \sqrt{g \cdot R}$ is remarkable. This suggests that the flow near the front of a bubble must be very close indeed to the theoretical flow near the front of a complete sphere in an inviscid fluid.
It will be noticed in figure 1.5 and in table 1.2 that C_D is much more variable than $U/\sqrt{R}$. These values of C_D are plotted as a function of θ_m in figure 1.6, and those found by integrating the observed pressures on the lenticular bodies in the wind tunnel are shown on the same figure.
It will be seen that there is considerable scatter, in the case of the bubbles, from the mean line representing the variation of C_D with θ_m, and that the line representing the values of C_D for the lenticular bodies is quite different from that representing the bubbles.

1.4 THE RELATIONSHIP BETWEEN VOLUME AND RATE OF RISE OF A BUBBLE

If all the bubbles were geometrically similar the dimension A could be expressed by

$$A = \alpha \cdot V^{\frac{1}{3}}\,, \tag{1.7}$$

where α would then be constant. If also the drag coefficient were constant, (1.5) shows that U would be proportional to $V^{\frac{1}{6}}$; in fact, (1.5) can be expressed in the form

$$UV^{-\frac{1}{6}} = \sqrt{2g/\pi\alpha^2 C_D} = 25.0/\alpha \cdot \sqrt{C_D}\,\text{cm.}^{\frac{1}{2}}\ \text{sec.}^{-1}. \tag{1.8}$$

To test how far the assumption that α and C_D and therefore $\alpha \cdot \sqrt{C_D}$ are constant, measurements were made involving thirteen bubbles rising in nitrobenzene and seventy-five in water. The results are shown in figure 1.7, where $UV^{-\frac{1}{6}}$ is plotted against $V^{\frac{1}{3}}$, U being expressed in cm./sec. and V in cm.^{3}. The experimental results of Miyagi and Hoefer with smaller bubbles are also shown. Though there is considerable scatter about the line

$$UV^{-\frac{1}{6}} = 24.8\,, \tag{1.9}$$

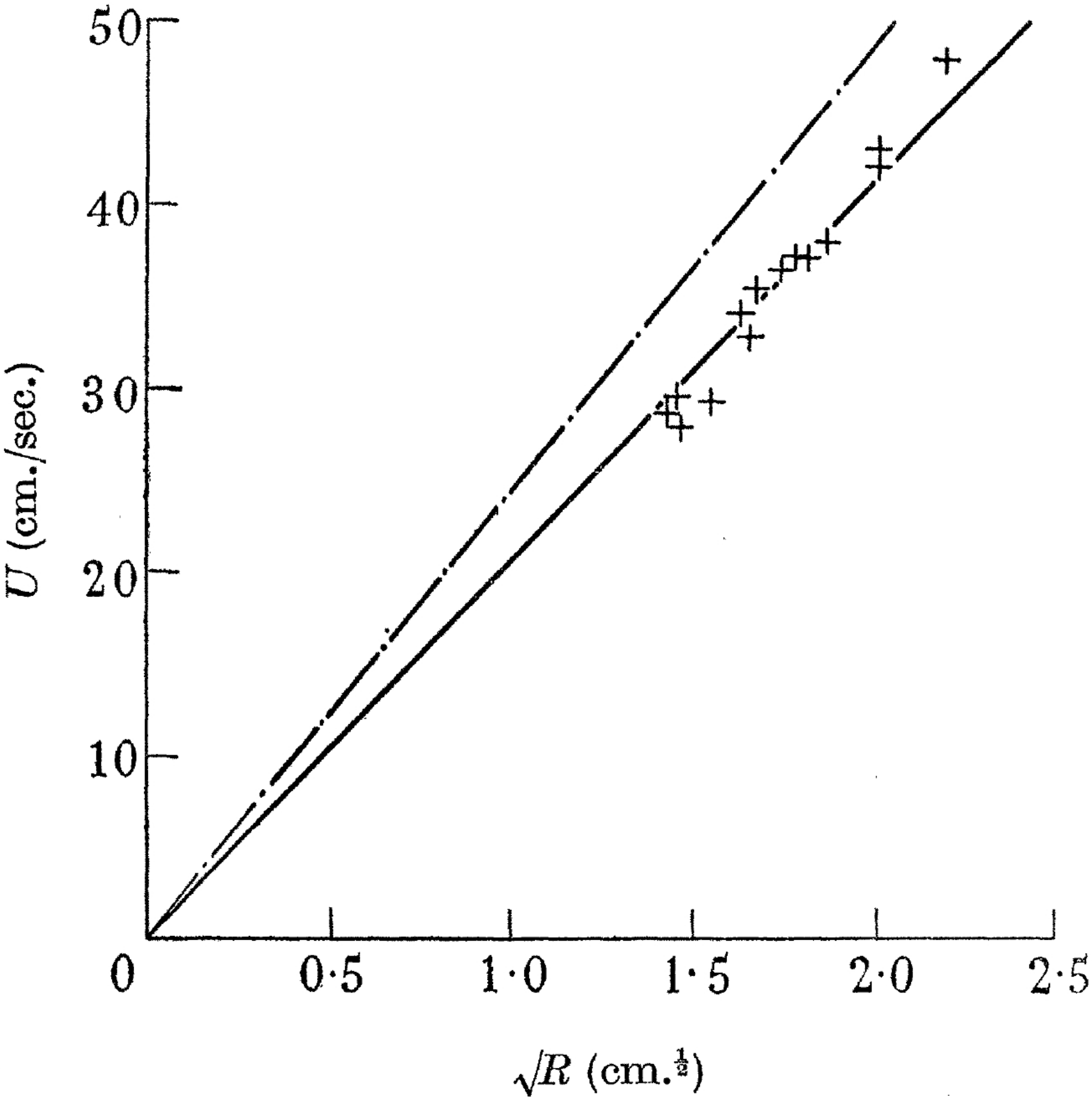

Figure 1.5
The relationship between the velocity of rise, U, of a bubble and the radius of curvature, R. + experimental values; —·– U = 0.78 $\cdot\sqrt{g \cdot R}$; — $U = \frac{2}{3} \cdot \sqrt{g \cdot R}$

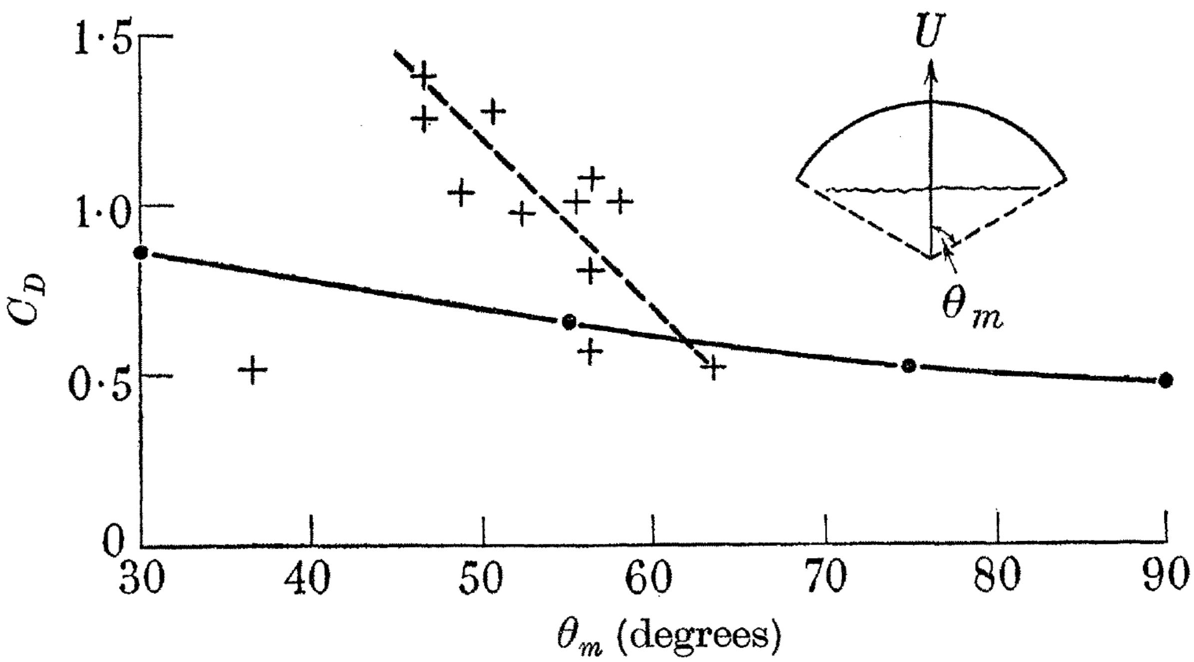

Figure 1.6
The experimental relationship between drag coefficient, C_D, and the semi-vertical angle, θ_m, subtended at the centre. + values for bubbles rising in nitrobenzene; • values for lenticular bodies in the wind tunnel

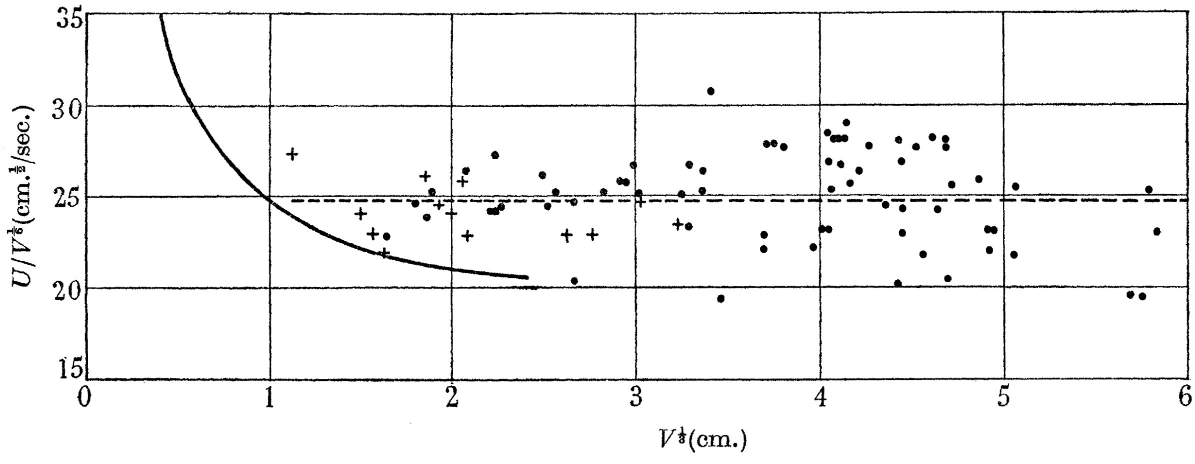

Figure 1.7
Experimental results for the velocity of rise, U, of a bubble of volume V. + bubbles in nitrobenzene; • bubbles in water; - - - $UV^{-\frac{1}{6}} = 24.8$ (mean value); — Miyagi and Hoefer results.

θ_m	30°	40°	50°	60°	70°	80°	90°
α	1.32	1.18	1.07	0.99	0.91	0.85	0.78

Table 1.3
Tabulated values of α for a series of values of θ_m

which represents the mean value giving equal weight to all the observations, figure 1.7 shows that there is no systematic variation in $UV^{-\frac{1}{6}}$ with V, and that the experiments in water and nitrobenzene give the same value of $UV^{-\frac{1}{6}}$. It is of interest to compare this experimental result with (1.8). In order that bubbles may ascend with the velocity $24.8 \cdot V^{\frac{1}{6}}$, which represents the mean of the experimental values,

$$\alpha \cdot \sqrt{C_D} = \frac{25.0}{24.8} = 1.0 \quad \text{approximately.} \tag{1.10}$$

It is of interest to note in table 1.2 that the mean value of C_D for the experiment in nitrobenzene is about 1.1. The value of α cannot be calculated unless the shape of the bottom of the bubble is known, but if the bubble were enclosed between a spherical upper surface and a flat lower one it can be shown that

$$\alpha^3 = \frac{3 \cdot \sin^3 \theta_m}{\pi \cdot (2 - 3 \cdot \cos \theta_m + \cos^3 \theta_m)} \,.$$

The values of α for a series of values of θ_m are shown in table 1.3.

It will be seen that in range $\theta_m = 46°$ to $\theta_m = 64°$, which contains all the experimental values in table 1.2, except that found for the smallest bubble, α is within 10 % of 1.0.

Example. Application to the bubble of gas released in a submarine explosion

When an explosive detonates under water, a mass of gas which is known, at any rate approximately, is suddenly produced. The volume of this bubble oscillates violently at first, but after a short time this oscillation ceases and the bubble rises and finally reaches the surface. It is of interest to calculate how fast such a bubble would rise if it behaved like those described in the foregoing experiments. A charge of say 300 lb. of amatol might be expected to produce, about $88 \cdot 10^{-7}$ cm.^{3} of gas at atmospheric pressure after the steam produced in the explosion had time to condense.

The formula (1.9) gives then

$$U = 525\,\text{cm./sec.} = 17.2\,\text{ft./sec.}$$

1.5 TURBULENCE IN THE WAKE BEHIND A BUBBLE

In the original photographs of bubbles in nitrobenzene, a region of turbulence is clearly shown behind the large bubble. This is due no doubt to some anisotropic optical property of nitrobenzene when subjected to viscous stresses. That such stresses exist could be inferred from the fact that, in the photograph shown in figure 1.1, the largest of the small bubbles in the wake of the large one is not spherical and is rapidly changing in shape. This bubble has a diameter of about 6 mm. Still smaller bubbles are less distorted, and one of diameter about 2 mm., seen to the left side of the 6 mm. bubble, is distorted so that its length to diameter ratio is about 1.1.
The rate of shear which might be expected to produce a distortion of this amount has been calculated by Taylor (1934). In the field of flow represented by the equations

$$u = C \cdot x, \quad v = -C \cdot y, \quad w = 0, \tag{1.11}$$

an air bubble of mean radius a would be pulled out so that

$$\frac{L-B}{L+B} = \frac{2C\mu a}{T} \tag{1.12}$$

where L and B are the length and breadth of the bubble and μ and T the viscosity and the surface tension of the liquid. For nitrobenzene, $\mu = 0.018$ poise, $T = 43.9$ dynes/cm., so that for the 2 mm. bubble, $a = 0.1$ cm., $L/B = 1.1$ and $(L-B)/(L+B) = 0.05$, giving

$$C = \frac{0.05 \cdot 43.9}{2 \cdot 0.018 \cdot 0.1} = 6.1 \cdot 10^2 \text{ sec.}^{-1}.$$

The rate W of dissipation of energy per cm.^{3} in the flow represented by equation (1.11) is

$$W = \mu \cdot \left\{ \left(\frac{\partial u}{\partial x}\right)^2 + \left(\frac{\partial v}{\partial y}\right)^2 \right\} = 2\mu C^2 = 1.34 \cdot 10^4 \text{ ergs/cm.}^3\text{/sec.}$$

If the rate of dissipation were constant through the wake, and if the wake extends over the whole of the region which appears disturbed in figure 1.1, namely, through a diameter of 5.9 cm. and a length of 3.8 cm., the total rate of dissipation in the wake is

$$\begin{aligned} & 1.34 \cdot 10^4 \cdot \text{volume of wake} \\ = & 1.34 \cdot 10^4 \cdot \frac{1}{4}\pi \cdot (5.9)^2 \cdot 3.8 \\ = & 1.4 \cdot 10^6 \text{ ergs/sec.} \end{aligned}$$

The total rate of dissipation would be known if the drag coefficient, C_D, of the large bubble were known. Since the density ρ of nitrobenzene is 1.2 g./cm.^{3}, whilst the velocity of rise, U, of the large bubble in this experiment was 36.7 cm./sec. and its maximum transverse dimension, $2A$, was 5.1 cm., the total rate of dissipation was

$$\begin{aligned}
&C_D \cdot \frac{1}{2}\rho U^2 \cdot \pi A^2 \cdot U \\
=&C_D \cdot \left\{\frac{1}{2} \cdot 1.20 \cdot 36 \cdot 7^3 \cdot \pi \cdot (2.55)^2\right\} \\
=&6.1 \cdot 10^5 \cdot C_D \ \text{ergs/sec.}
\end{aligned}$$

Since C_D is found to be of the order of 1.0 (see table 1.2), it will be seen that the rate of dissipation which would distort the bubbles by the observed amount is of the same order as that deduced from the rate of rise.
For the largest of the small bubbles in the wake, viscous stresses would produce such a distortion that the formula (1.12) would not be expected to apply.

2 PART II. EMPTYING WATER FROM A VERTICAL TUBE

2.1 THEORETICAL DISCUSSION

It has been seen that large bubbles in water assume a form which is very nearly the lenticular volume contained between a sphere and a horizontal plane cutting it above its centre. The pressure distribution over the spherical surface is found experimentally to be approximately the same as that calculated for a complete sphere moving in an ideal fluid. This pressure, together with the hydrostatic pressure due to gravity, leads to a uniform surface pressure when the velocity of rise, U, is

$$U = \frac{2}{3} \cdot \sqrt{g \cdot R},$$

R being the radius of the upper surface of the bubble.

It has been found that when the rate of rise and radius of curvature of large bubbles have been measured simultaneously, these quantities do in fact very nearly satisfy this relationship.

This result depends on the observed fact that the pressure distribution over the forward portion of a lenticular shaped body is nearly the same as the theoretical distribution over a complete sphere. This empirical observation makes it possible to have a partial understanding of why it is that the upper surface of a large rising bubble is so nearly spherical, but it does not lead to a complete understanding because the relationship between the shape of the bubble and the pressure distribution over its surface is not understood. The main difficulty in this matter is to obtain a correct description of the currents in the wake which follows the nearly flat lower surface of the bubble.

For this reason we may consider the case where the bubble is confined inside a circular tube. In this case the fluid can run round the outside of the bubble and remain as a layer running down the surface of the tube and falling freely under gravity. In this case it is not necessary for the bubble to have a lower surface. The tube, in fact, is open to the atmosphere at its lower end. The problem thus posed is capable of being solved completely. The question to be answered is “How fast will the air column rise in a vertical tube with a closed top when the bottom is opened?” or, alternatively, “How fast will a vertical tube with a closed top empty itself when the bottom is opened?”

If U is the velocity of rise of the air column in a tube of radius a, the flow can be brought to a steady motion by giving the whole system a downward velocity U. The top of the air column is now at rest, and if x is the depth below this, the condition which must be satisfied at points on the free surface of the air column is

$$q^2 = 2 \cdot g \cdot x\,, \tag{2.1}$$

where q is the velocity of the liquid and g is the acceleration due to gravity. The problem is, therefore, to find the shape of a body of revolution which if inserted in a circular tube will leave a space through which a perfect fluid could flow so that the velocity at its surface would be proportional to $\sqrt{x}$. This problem could be solved by relaxation methods, but a rough approximation to the flow near the top of the air column may be obtained as follows: The velocity potential

$$\phi = e^{K_n \cdot x/a} \cdot J_0\left(K_n \cdot r/a\right) \tag{2.2}$$

represents a flow contained in a tube of radius a provided K_n is a root of the equation $J_1(z) = 0$. Here J_0 and J_1 are Bessel functions. The flow has the property that it dies away to zero, when x has large negative values.
The flow represented by

$$\phi = -U \cdot x + \sum_n A_n \cdot e^{K_n \cdot x/a} \cdot J_0\left(K_n \cdot r/a\right) \tag{2.3}$$

and by the Stokes stream function

$$\psi = -\frac{1}{2} \cdot Ur^2 + r \cdot \sum_n A_n \cdot e^{K_n \cdot x/a} \cdot J_0\left(K_n \cdot r/a\right) \tag{2.4}$$

has the property that it has uniform velocity U for large negative values of x, and that the radial velocity is zero at $r = a$. The pressure condition which must be satisfied on the surface $\psi = 0$ is

$$\left(\frac{\partial \phi}{\partial x}\right)^2 + \left(\frac{\partial \phi}{\partial y}\right)^2 = 2 \cdot g \cdot x\,. \tag{2.5}$$

It seems unlikely that an analytical solution of this problem could be found but a rough approximation to the flow near the top of the air column might be obtained by using only one term of the series in (2.3). The lowest root of $J_1(z) = 0$ is 3.832, so that as a first approximation (2.3) may be taken as

$$\phi = -U \cdot x + A_1 \cdot e^{3.832 \cdot x/a} \cdot J_0\left(3.832 \cdot r/a\right)\,, \tag{2.6}$$

and (2.4) as

$$\phi = -\frac{Ur^2}{2} + A_1 r \cdot e^{3.832 \cdot x/a} \cdot J_1\left(3.832 \cdot r/a\right) . \tag{2.7}$$

The surface of the bubble is $\psi = 0$. In order that $x = 0$ may be the vertex of the air column it is necessary that the coefficient of r^2 in the expansion of ψ near the origin shall be zero. This condition is satisfied if

$$A_1 = \frac{U \cdot a}{3.832} . \tag{2.8}$$

It is clearly impossible to satisfy the pressure condition (2.1) at more than one point when only one term in the series expansion (2.3) is used. Assume that (2.5) is satisfied at the point if $\psi = 0$ when $r = \frac{1}{2}a$. The value of x at this point is found by setting

$$A_1 = U \cdot a/3.832, \quad r/a = \frac{1}{2}, \quad \psi = 0 \quad \text{in (2.5)} .$$

The value of $J_1\left[\frac{1}{2}(3.832)\right]$ is 0.580, so that (2.7) gives

$$e^{3.832 \cdot x/a} = \frac{3.832}{4(0.580)} = 1.65, \quad \text{and} \quad \frac{x}{a} = 0.131 .$$

Since $J_0\left[\frac{1}{2}(3.832)\right]$ = 0.273, (2.5) gives

$$\frac{2 \cdot g \cdot a}{U^2}(0.131) = \{1 - (1.65)(0.273)\}^2 + \{(0.580)(1.65)\}^2 ,$$

hence

$$\frac{U^2}{g \cdot a} = 0.215$$

or

$$U = 0.464 \cdot \sqrt{g \cdot a} . \tag{2.9}$$

This very rough approximation to the flow might be improved by using more terms in the series in (2.3). It would then be possible to satisfy the pressure condition at as many points as the number of terms taken in the series of (2.3), the values of x/a would be calculated for each assumed value of r/a, and the final equation for determining $U/\sqrt{g \cdot a}$ would be left. The numerical work, however, would be very heavy, and a relaxation method would probably be more satisfactory.

$2a$ (cm.)	1.23	2.16	7.94
U (cm./sec.)	9.8 to 10.15	14.5 to 15.2	29.1 to 30.6
$U/\sqrt{g \cdot a}$	0.40 to 0.41	0.447 to 0.468	0.466 to 0.490
$\frac{U \cdot a}{\nu} = Re$	600	1,600	12,000
	calculated value, $U/\sqrt{g \cdot a}$ = 0.464		

Table 2.1
Reynolds number calculated for bubbles within a tube of radius a

2.2 EXPERIMENTS ON EMPTYING VERTICAL TUBES

To find out whether the flow postulated in the above calculations can actually occur, a long glass tube was erected vertically over a sink in the Cavendish Laboratory. It was filled by placing the lower end in a basin of water and applying suction at the upper end through a rubber tube till the water-level reached the top. The rubber tube was then closed. To make an experiment the basin at the lower end was suddenly removed and a bubble was seen to run up the tube, the water emptying itself by running down the wall and pouring out from the bottom in the form of a tubular curtain of water. The photograph (figure 2.1), shows a flash-picture of the bubble running up a tube 7.94 cm. diameter. This tube was surrounded by a flat-sided glass box filled with water in order to reduce distortion by refraction.

It will be seen that the flow assumed in the analysis actually takes place. The thickness of the sheet of water that runs down the wall can be seen in the photograph, and measurements show that except close to the vertex this thickness is, as would be expected from (2.1), inversely proportional to the square root of the depth below the vertex.

Experiments were made with three tubes each about 180 cm. long and of diameters 1.23, 2.16 and 7.94 cm. The upward velocities of the tops of the bubbles were observed by timing their passage past horizontal marks with a stop-watch. The observed velocities together with the corresponding values of $U/\sqrt{g \cdot a}$ are given in table 2.1.

It will be seen that the values of $U/\sqrt{g \cdot a}$ are nearly constant but tend to rise slightly with diameter. This is probably an effect of viscosity. The Reynolds numbers associated with the bubbles are given in table 2.1. It will be seen that the Reynolds number associated with the largest tube is so great that it might be expected that the effect of viscosity would be negligible in that case. It is remarkable that the very rough theory given above yields the value 0.464 for $U/\sqrt{g \cdot a}$, which is very close to the range 0.466 to 0.490 which was observed experimentally with the largest tube.

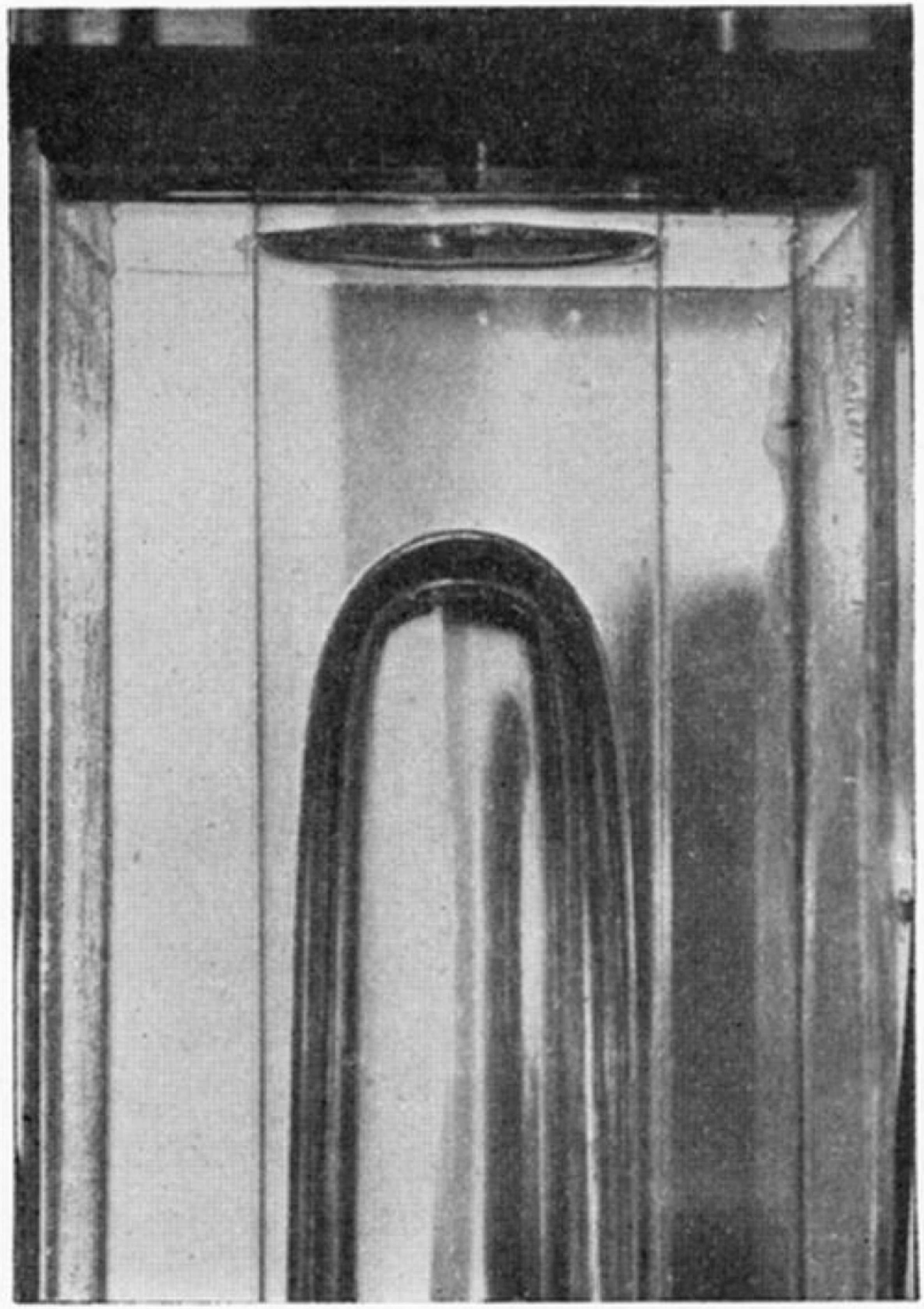

Figure 2.1
Emptying a glass tube 7.9 cm. diameter

x/a	1.71	3.43	5.14	6.17
t/a	0.171	0.123	1.103	0.093
$\beta = 2 \cdot \sqrt{2} \cdot (t/a) \cdot \sqrt{x/a}$	0.63	0.64	0.66	0.65

Table 2.2
Values of t/a and x/a, where t is the time the bubbles pass past a horizontal mark

2.3 MEASURED PROFILE

The profile of the bubble taken from a photograph similar to figure 2.1 is shown in figure 2.2. After passing the rounded top of the bubble, the water concentrates into a sheet near the wall. At a depth of about 1.5 a below the vertex the horizontal component of flow becomes so small that the vertical component, U, may without appreciable error be taken as equal to q. The equation to the part of the profile below $x = 1.5\ a$ is therefore approximately

$$U \cdot \pi \cdot a^2 = \pi q \cdot \left(a^2 - r^2\right) = \pi \cdot \left(a^2 - r^2\right) \cdot \sqrt{2 \cdot g \cdot x}\,,$$

or if t is written for $(a - r)$, the thickness of the layer of water running down the inside of the tube, and $U = \beta \cdot \sqrt{g \cdot a}$,

$$2\frac{t}{a} - \frac{t^2}{a^2} = \beta \cdot \sqrt{\frac{a}{2 \cdot x}}\,,$$

and since t is small compared with a,

$$\beta = 2 \cdot \sqrt{2} \cdot \left(\frac{t}{a}\right) \cdot \sqrt{\frac{x}{a}}\,.$$

By measuring t and x in figure 2.2 therefore it should be possible to find β for comparison with the value deduced from velocity measurements and given in table 2.1. Corresponding values of t/a and x/a are given in table 2.2.

It will be seen that the values of $t \cdot \sqrt{x}$ are nearly constant, but the value of β deduced from them is much larger than that found by measuring the velocity of the bubble. The difference may be due to the fact that the existence of the boundary layer at the inner wall of the tube was not considered, so that the downward flow estimated by measuring t and assuming that U is uniform through the layer gives rise to an overestimate. Another cause which gives rise to an overestimate of t is the refraction of the glass tube, an error which is not completely eliminated by surrounding it with a parallel-sided glass box, filled with water.

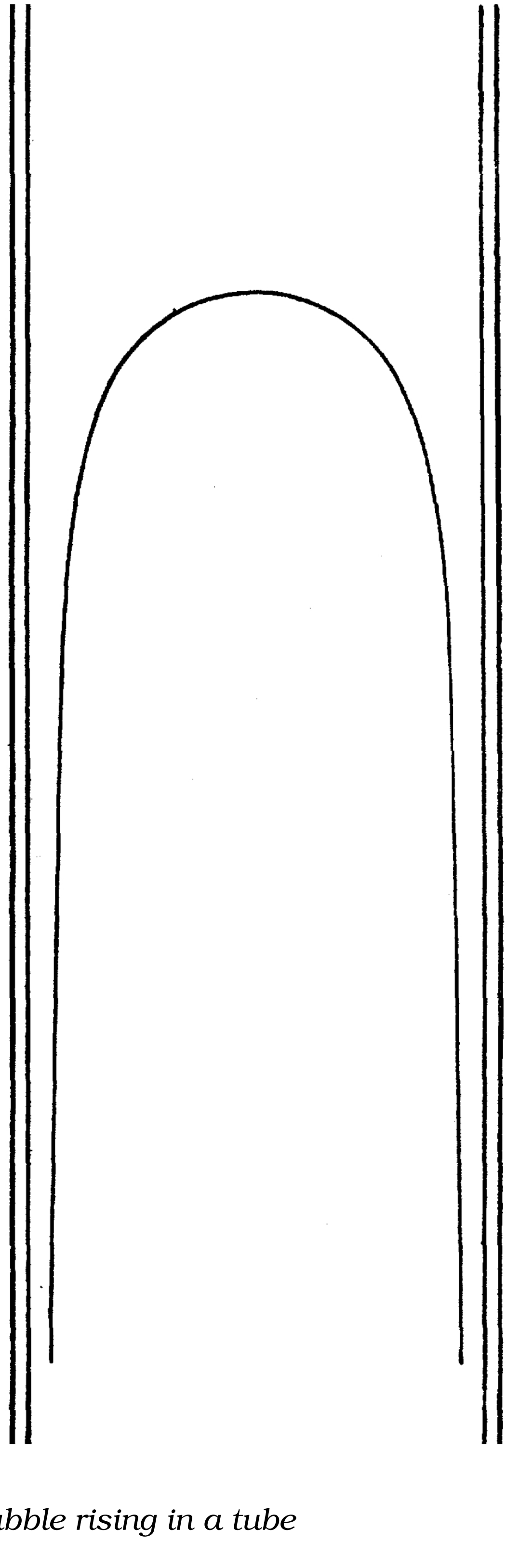

Figure 2.2
Profile of a bubble rising in a tube

3 REFERENCES

Allen, H. S. 1900 *Philosophical Magazine* **50**, 323, 519.
Hoefer, K. 1913 *Zeitschrift des Vereins Deutscher Ingenieure* **57**, 1174.
Miyagi, O. 1925 *Philosophical Magazine* **50**, 112.
Miyagi, O. 1925 *Tohoku Imperial University, Technol. Report*, **5**, 135.
Miyagi, O. 1929 *Tohoku Imperial University, Technol. Report*, **8**, 587.
Taylor, G. I. 1934 *Proceedings of the Royal Society A*, **146**, 501.